

IPACK2001-15740

FLO/STRESS: AN INTEGRATED STRESS SOLVER FOR THE CFD TOOL FLOTHERM

M. Warner

School of Computing and
Mathematical Sciences
The University of Greenwich
30 Park Row, Greenwich, London
SE10 9LS, U.K.
email: matt.warner@flomerics.co.uk

J. Parry

Flomerics Limited, 81 Bridge
Road, Hampton Court, Surrey,
KT8 9HH, UK
email:
john.parry@flomerics.co.uk

C. Bailey

School of Computing and
Mathematical Sciences
The University of Greenwich
30 Park Row, Greenwich, London
SE10 9LS, U.K.
email: c.bailey@gre.ac.uk

C. Marooney

Flomerics Limited, 81 Bridge
Road, Hampton Court, Surrey,
KT8 9HH, UK
email:
chris.marooney@flomerics.co.uk

H. Reeves

Flomerics Limited, 81 Bridge
Road, Hampton Court, Surrey,
KT8 9HH, UK
email:
hugh.reeves@flomerics.co.uk

K. Pericleous

School of Computing and
Mathematical Sciences
The University of Greenwich
30 Park Row, Greenwich, London
SE10 9LS, U.K.
email: k.pericleous@gre.ac.uk

ABSTRACT

The future of many electronics companies will depend to a large extent on their ability to initiate techniques that bring schedules, performance, tests, support, production, life-cycle-costs, reliability prediction and quality control into the earliest stages of the product creation process. An important question for engineers who are responsible for the quality of electronic parts such as circuit card assemblies (CCAs) during design, production, assembly and after-sales support is: What is the impact of temperature on the performance and reliability of the components and hence the whole system?

At present, thermal and thermomechanical analyses are usually undertaken using different software tools that require separate model build and meshing. This leads to a large investment in time, and hence cost, to undertake each of these simulations. This paper details the development of a new thermal-stress module FLO/STRESS™, integrated into the FLOTHERM™ CFD software, thereby using a common data model and user interface. A discussion of its use within the product design process is given, followed by an example of this integrated modeling approach for a CBGA component, comparing the results with previously published reliability data.

Keywords: Reliability Analysis, Multiphysics Modelling

INTRODUCTION

Increasing global competition is a significant factor impacting the design of modern electronic products. While the product development time for electronic systems in the early 1980s was often years, portable computing and consumer products for example have today a time-to-market of only a few months. These rapid times-to-market do not leave room for time-consuming trial and error approaches that have been the normal practice in the past. Today, experimentally validated computational modeling has become the preferred choice for rapidly carrying out numerous 'what-if' studies during design. At present such modeling technologies do not, in general, provide coupled solutions for thermal and mechanical issues. For example, at the system level an engineer may be interested in predicting the flow and temperature fields throughout the system, and then want to use these results to calculate the stresses and strains within a circuit board assembly or a chip package, (due to the thermal miss-match between different materials). The need for such integrated modeling approaches is

emphasized in the Semiconductor Industry Association's 1997 Roadmap document [1], which states:

“Developments in chip size, packaging techniques, power dissipation, and switching speed require new simulation tools that treat thermal, mechanical and electrical effects self-consistently.”

This roadmap focuses primarily on issues associated with semiconductor manufacture and packaging. However, the need for a self-consistent solution of thermal, mechanical and electromagnetic effects extends from the package level up to the system level.

From a mechanical perspective, an electronics package is a composite structure that undergoes thermal loadings. Thermal stresses and strains occur due to the mismatch in thermal expansion of the different materials from which the package is manufactured. The determination of thermal stresses and strains in electronics packaging is a very difficult task because of its complex geometry and materials of construction [2]. The influence of both thermal and thermo-mechanical effects on equipment reliability is now widely recognized, and physics-of-failure based approaches to the design, production and reliability assessment of electronics equipment are being adopted [3,4].

To be successful, the design of today's electronic systems requires the adoption of a multi-disciplinary approach early within the design process, whereby electrical, thermal, mechanical and packaging engineers collaborate to make the necessary design trade-offs. To avoid discovering many problems late in the design process, design evaluations made throughout the design process would benefit from simulation tools that provide fast, coupled thermal and mechanical solutions. However, there are no coupled CFD and FE analyses available that are dedicated to design within the electronics packaging industry.

Flomerics is developing novel technologies that provide a unified modeling framework for thermal, mechanical, and electromagnetic predictions. This multi-physics methodology is based on numerical algorithms using current best-in-class techniques that are integrated in an efficient and robust manner. The tight integration between modules provides users with a common user interface that facilitates the ease of model building and the interpretation of the results. By focussing on electronics applications, integrated 'Design Class' analysis software can be created, tailored to the physical analysis of electronics systems. As will be shown later in this paper, this can achieve fast, practical analysis of the stress effects early in the design process.

INTEGRATION OF THE STRESS MODULE

The FLOTherm – FLO/STRESS integration enables a stress analysis of an electronic assembly to be performed within the thermal design software environment. The stress analysis module uses the CFD model, mesh and temperature results of

the selected assembly. Within this assembly, only the mesh in the solid regions is of interest for the stress calculation. Figure 1 summarizes the input data and results generated by the CFD and FE analyses. Geometry, grid and temperature information is passed from the CFD solver to the FE solver at the end of the CFD calculation. Results from the stress analysis are available for post-processing in FLOTherm, making the integration seamless within a common shared software environment.

The stress equations solved in FLO/STRESS are discretized using traditional finite element procedures, where the change in temperature predicted by the thermal analysis is used to calculate the solid deformation. The stress solver uses 8-node brick elements to replicate the CFD mesh within the solid regions of the assembly. Care has been taken to ensure that very little extra work is required to provide the capability to undertake a fast stress calculation based on the predicted thermal gradients. No extra model build or meshing is required. The only additional input is the relevant materials data and boundary conditions required for the stress calculation. Material properties can be input as isotropic or orthotropic, and can be temperature-dependent.

Design Class Analysis Software

It is envisaged that the FLO/STRESS FEA module will be used within FLOTherm in a manner equivalent to that in which specifically designed FE packages are used within CAD and solid modeling packages. Such packages include visualNastran Desktop FEA, COSMOS/DesignStar and COSMOS/WORKS. These packages allow easy-to-use structural analysis for non-FE specialists within the mechanical design process. This FEA module is intended for use in electronics product design rather than qualifying novel packaging technologies. A linear elastic FEA capacity within FLOTherm will enable design engineers to perform fast, first-order accurate thermomechanical calculations within the thermal design process.

Product Design vs. Technology Qualification

In technology qualification, the business and technical risks associated with a new technology are assessed ahead of their use in products, using a range of analysis techniques. Recent examples of novel technologies include BGAs, flip chip and lead-free solder. The focus is on learning as much as possible about the technical and business issues of deploying the new technology across the company's product range and the lead times are relatively long. Consequently, engineers and scientists engaged in this activity, being the traditional users of finite element technology, are able to use the most sophisticated analysis techniques available in high-end tools. For example, a full visco-plastic analysis over several temperature cycles has been used to investigate the thermomechanical behavior of a single solder ball as a function of its geometry and composition [5], and to investigate the influence of voids. [6].

In product design, the business objective is to gain confidence in the design. Intense competition with fast design

cycles promotes an evolutionary approach to product design, where incremental changes are made to the design to reduce business risk. Often, no new technologies are deployed, so changes in the relative performance and reliability of the system arise directly from changes to the design. Consequently, investment is required to ensure several iterations of a particular design can be assessed in a matter of a few weeks. Emphasis is more on performing a range of analyses that can be repeated and refined during each design iteration, than on obtaining the most accurate result in any single analysis. Cost effective trade-offs have to be struck.

Simplification and partitioning of the problem across different levels of packaging are used to make the analyses more tractable, particularly early in the design cycle, with detail added as more complete information becomes available. A system-level thermal analysis will have a relatively good representation of the thermal environment experienced by a particular CCA, but much of the physical detail of the board will be approximated. By contrast, a board-level thermal analysis will use an idealized representation of the thermal environment but can consider the board in greater detail. Neither model is a true representation of the system, but together the two models can provide the designer with a far better understanding of the behavior of the design, than could be obtained from either one of them.

Once an adequate thermal design has been achieved, time pressure often prevents further analysis being performed. Simple design rules provide some confidence, but ideally, the analyses should be extended to investigate the thermo-mechanical performance of the design and particularly the CCAs. The proximity of neighboring components can significantly increase the temperature cycle experienced by the package-board interconnect, and can also locally stiffen the

board, reducing the extent to which board warpage can reduce the strain on the package interconnect. These effects generally conspire to reduce the life of a solder joint. If not recognized during design, this may manifest itself during accelerated testing, delaying the release of the product, or worse.

Performing a thermomechanical analysis of a whole board assembly is generally impractical. However performing an analysis of a single component, including a small section of the board on which it is mounted is quite feasible. Thus, a board-level or system-level thermal analysis can provide the thermal environment for several thermomechanical analyses. The process of performing a stress analysis within the FLOTHERM thermal analysis is illustrated below in the form of two examples.

ILLUSTRATIVE EXAMPLES

The two examples chosen employ a model of the Motorola PowerPC™ 604 C4/CBGA on a 2-inch test coupon. For the first example, this assembly is located within a wind tunnel, the die is the only heat source in the system. For the second example, the entire assembly is located within a temperature cycling chamber, the die produced no heat of its own, and thus the temperature is uniform throughout the assembly.

For the Motorola PowerPC™ 604 C4/CBGA, the C4 interconnection provides both the electrical and the mechanical connections for the die to the ceramic substrate. After the C4 solder bumps are reflowed, epoxy (encapsulant) is under-filled between the die and the substrate. The package substrate is a 21mm x 21mm multi-layer co-fired ceramic. The package-to-board interconnection is by an array of 16 x 16 orthogonal Pb90/Sn10 solder balls on a 1.27mm pitch.

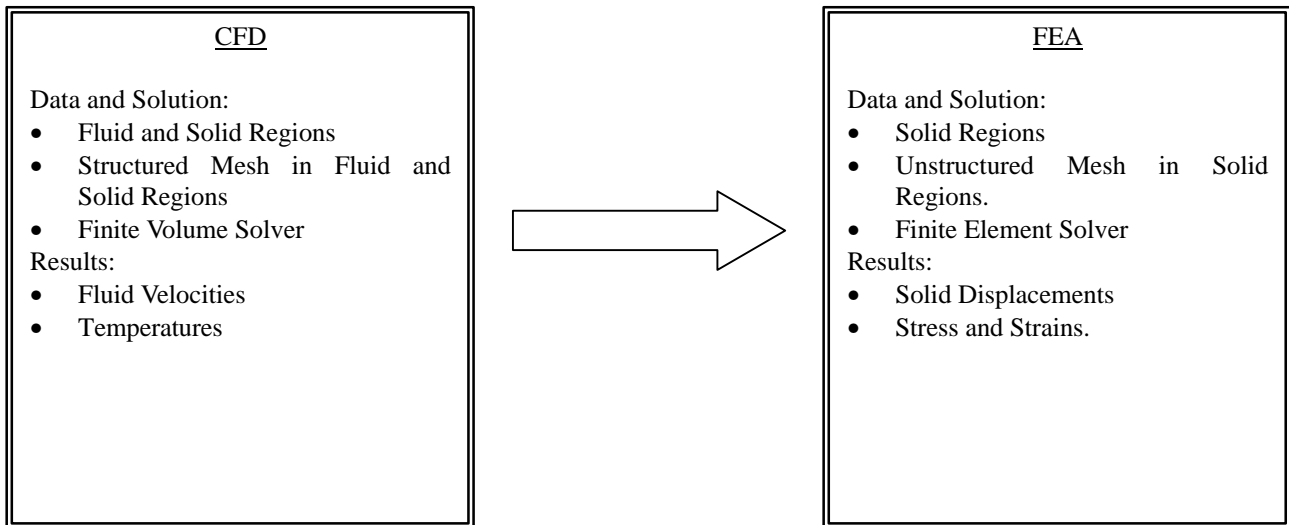


Fig. 1: Integration between FLOTHERM and FLO/STRESS

Modeling Approach

The detailed model of the package was constructed in FLOTHERM. The package was constructed from conducting cuboid blocks representing the die, C4/underfill, co-fired ceramic substrate, and the ball grid array. Figure 2 shows the test assembly in the wind tunnel.

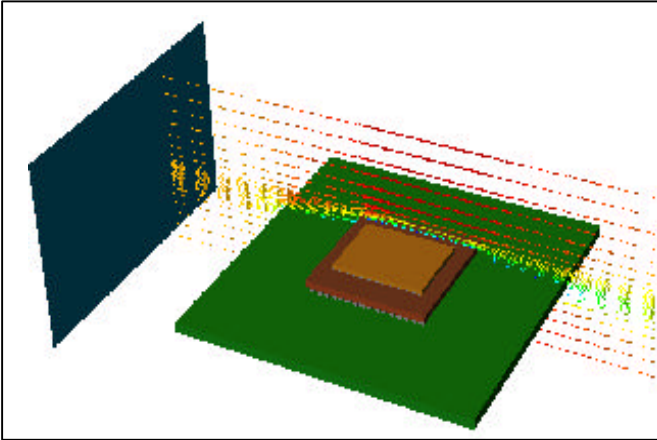


Fig. 2: Model Package on test board in wind-tunnel.

During assembly of the C4/CBGA package to the board, the higher melting point Pb90/Sn10 solder balls do not collapse [7] but are soldered to the board, as they are to the package, with lower melting point Sn63/Pb37 solder. To a first approximation, the Pb90/Sn10 solder ball is a sphere encased within a cylinder of Sn63/Pb37 solder. A schematic giving a cross-section through the model of the package is shown in Figure 3.

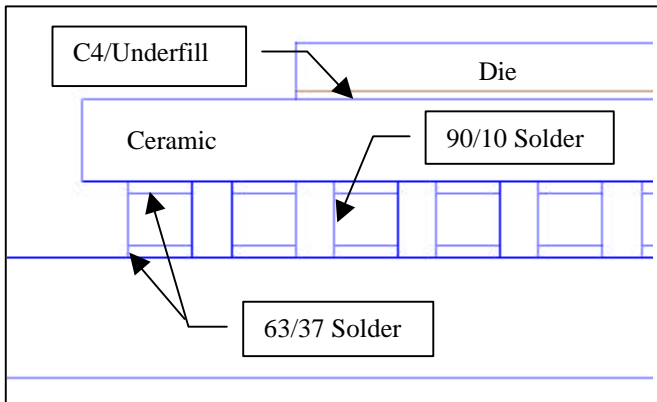


Fig. 3: Schematic of C4/CBGA and PCB

In this analysis, the solder joint is modeled as cuboidal, having the same cross-sectional area and height as the cylinder. The volume of the Pb90/Sn10 and Sn63/Pb37 solder are also preserved, with the Sn63/Pb37 solder being distributed equally above and below the Pb90/Sn10 solder. This approach is similar to the global-local modeling techniques used to simulate the thermal stress at the package and solder bump levels [8].

EXAMPLE 1: WIND TUNNEL TESTING

Model Description

The detailed model of the package and test board [9] was mounted in a computational wind tunnel and the conjugate steady state heat transfer solved. The wind tunnel had a cross-sectional area of 2581mm² (50.8mm x 50.8mm) and a fixed velocity of 1.0 m/s.

Material Properties

The properties of the materials used in the model are given in Table 1. In the model, the material properties for Pb95/Sn5 were used as a close approximation for Pb90/Sn10.

Table 1: Material Properties Used in Model

Material	Thermal Conductivity (W/mK)	CTE (ppm)	Young's Modulus (GPa)	Poisson's Ratio (-)
PCB	5.0	15.0	18.2	0.25
Pb95/Sn5	35.5	27.8	24.0	0.4
Sn63/Pb37 (20°C)	50.6	24.0	30.2	0.4
(140°C)	50.6	24.0	19.7	0.4
Ceramic	16.5	6.7	300.0	0.23
C4/U'fill	0.8	52.0	1.0	0.3
Silicon	120	2.3	162.0	0.28

For the PCB, the thermomechanical properties used are those for FR4. For simplicity, isotropic mechanical properties were used for the PCB, although this is not a limitation of the FLO/STRESS module. The thermal conductivity is that for a board containing approximately ½Oz copper. The effective (through plane) thermal conductivity used for the C4/Underfill was calculated from data on the size and number of the C4 bumps and the thermal conductivity of the solder and the underfill epoxy [9]. In this illustrative work the thermomechanical properties used for the C4/Underfill are those for the underfill epoxy.

Stress Analysis

In order to perform the stress calculation an assembly in the model is targeted, to which constraints are applied and a stress-free temperature defined for each object. The stress-free temperature for all objects was assumed to be 170°C in this analysis, being the cure temperature for the C4 underfill.

After performing the thermal calculation in FLOTHERM, the thermally induced stresses were solved using FLO/STRESS. The computational overhead required is given in Table 2. In this particular example, the stress analysis requires less computational time than that for the thermal analysis. The primary reason for this is that the mesh is much smaller, since displacements are only calculated in the solid regions of the target assembly within the model. Another factor determining the relative solution times is the number of variables solved for:

the CFD analysis solves for five variables, whereas the FE analysis solves for three.

Table 2: Model Characteristics

	Thermal Model	Thermomechanical Model
Number of cells / elements	225600	102400
Relative solution time	1.0	0.22

Once the model had been solved, results were post-processed using FLOMOTION™.

Results

The results can be seen to be qualitatively correct. Figure 4 shows the temperature in the assembly. The effect of the wind tunnel in cooling the assembly can be clearly seen, as flow passes from left to right in the plot.

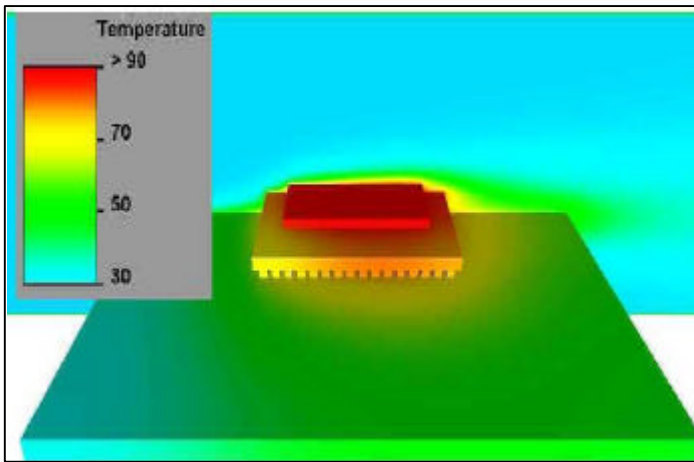


Fig. 4: Surface Temperatures (°C) on Package and Board. Air temperature shown on centerline.

The temperature changes gave rise to deformation in the assembly and hence stress due to the thermal mismatch in materials. The thermal mismatch between the substrate and the solder joints is greater than the thermal mismatch between the solder joints and the PCB. This resulted in peak von Mises stresses at the solder-substrate interface (figure 5).

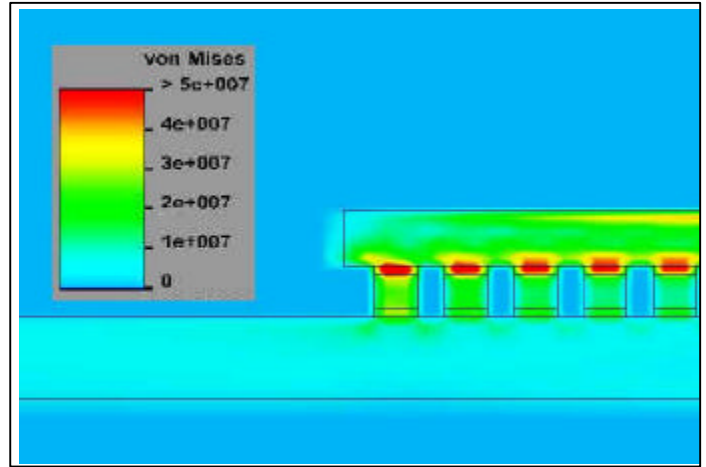


Fig. 5: Peak von Mises stress (N/m²) in solder joints

Figure 6 shows the stress magnitudes at the solder-package interface. The influence of the wind tunnel in cooling the assembly can be seen again, with the stresses being higher at the leading edge (on the left of the plot).

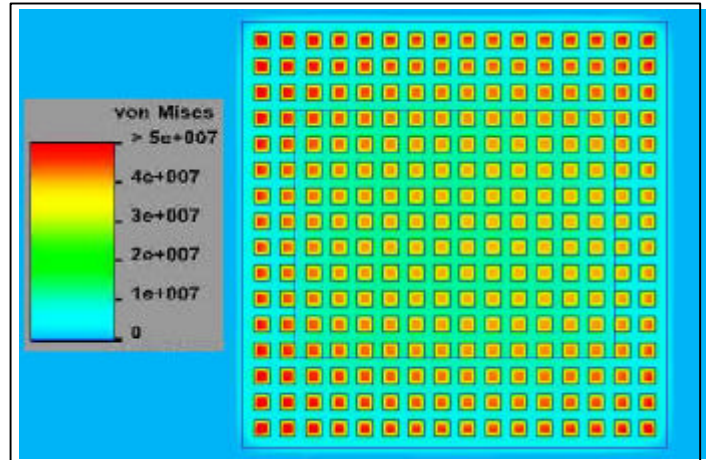


Fig. 6: von Mises stress (N/m²) in solder-substrate interface

Prediction of the highest stresses in the solder joints adjacent to the package substrate is expected. An investigation into the behavior of a CBGA 625 package during temperature cycling revealed that when the package was subjected to rapid thermal cycling from -55°C to 125°C failures mainly occurred at the package-solder joint interface, being driven by local stress conditions [10].

EXAMPLE 2: RELIABILITY PREDICTIONS

Model Description

To gain further confidence in the stress predictions, the model was modified to be consistent with the accelerated tests performed by Gerke and Kromann [11] on the same package, and the number of cycles to failure was predicted. These were compared with accelerated test results and a simple analytical model. The FLOTERM model consisted of a CBGA package mounted on a PCB. In particular, the PCB was modeled in detail, as FR4 with two 1Oz copper planes in the center to simulate power and ground and two ½Oz copper planes on top and bottom to simulate the signal layers.

Material Properties

FR4 was modeled as an orthotropic material. Temperature dependent properties for Sn63/Pb37 and Pb90/Sn10 were also included in the model.

Table 3: Material Properties for Reliability Predictions

Material	CTE (ppm)	Young's Modulus (GPa)	Shear Modulus (GPa)	Poisson's Ratio (-)
FR4 (in-plane)	22.8	12.8	2.57	0.13
FR4 (out-of-plane)	73.0	6.5	1.96	0.50*
Copper	16.7	117.0	-	0.34
Ceramic	6.7	300.0	-	0.23
C4/Underfill	52.0	1.0	-	0.3
Silicon	2.3	162.0	-	0.28
Sn63/Pb37 (22°C)	25.4	43.251	-	0.3628
(50°C)	26.1	41.334	-	0.3650
(75°C)	26.7	39.445	-	0.3700
(100°C)	27.3	36.854	-	0.3774
Pb90/Sn10 (0°C)	27.8	23.984	-	0.4
(50°C)	28.2	22.650	-	0.4
(100°C)	28.6	21.317	-	0.4

* major Poisson's ratio.

1) Accelerated Test Results

Accelerated thermal test procedures have been used to predict solder fatigue life for typical CBGA and CQFP packages in typical computer applications [11]. The cycles to failure for 0.01% sample failure of the CBGA package at operating conditions were extracted from solder fatigue life projections published in Gerke and Kromann (1999) [11]. These results were estimated using an acceleration factor developed by Norris and Landsberg [12]:

$$AF = \left(\frac{\Delta T_l}{\Delta T_f} \right)^{1.9} \times \left(\frac{f_f}{f_l} \right)^{\frac{1}{3}} \times \exp^{1414 \times \left(\frac{1}{T_f} - \frac{1}{T_l} \right)} \quad (1)$$

Where: ΔT = temperature variation
 f = cycle frequency (cycles/day)
 T = maximum temperature (K)

Subscripts l and f denote lab and field conditions

2) FLO/STRESS Model Predictions

Three temperature ranges were used to simulate typical operating On-Off cycles: 20°C, 35°C and 50°C.

Figure 7 shows the shear strain in the solder joints predicted for the 35°C cycle. The peak shear strain occurred at the solder-substrate interface of the corner solder ball.

Under certain conditions, the total shear strain calculated in a linear elastic FLO/STRESS analysis can be considered to be equivalent to the plastic shear strain. If the calculated strain is much greater than the elastic limit, then the elastic strain in the solder will be a small proportion of the total strain. This approach is employed by Getkin *et al.* (1997) [13] to predict solder joint reliability from a linear elastic FE analysis.

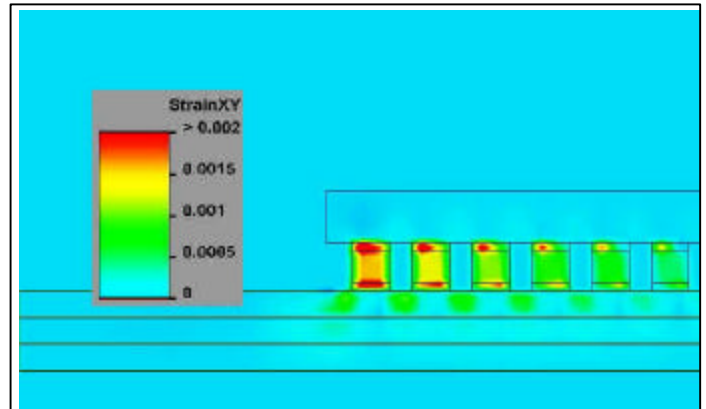


Fig. 7: Peak shear strain in solder joints during 35°C cycle.

For the 35°C cycle, a peak shear strain of 0.226% was predicted in the solder-substrate interface. Figure 8 also shows that the strain predicted throughout the solder-substrate interface is well in excess of the elastic strain limit of 0.02% for the solder joints at room temperature [13]. Thus, for a first approximation, this total shear strain may be considered equal to the plastic strain, making it possible to apply the Coffin-Manson equation to predict the cycles to failure:

$$N_f = \frac{1}{2} \left(\frac{2e_f}{g_p} \right)^m \quad (2)$$

Where: ϵ_f = fatigue ductility coefficient
 γ_p = shear strain
 m = ductility exponent

The peak shear strains were observed in the Pb90/Sn10 solder. The values used for this calculation were $\epsilon_f = 0.325$ and $m = 2.2$.

The Coffin-Manson model predicts the cycles to failure at 50% samples failed. A Weibull failure distribution can be used [14] to modify the model to predict cycles to failure at x% of population failed:

$$N_f(x\%) = N_f(50\%) \left(\frac{\ln(1-0.01x)}{\ln(0.5)} \right)^{1/\beta} \quad (3)$$

Where: β = Weibull shape parameter.

The cycles to failure for 50% sample failure were calculated using Equation 2 and extrapolated to 0.01% sample failure using Equation 2. Sensitivity to the value of β was also investigated.

3) Analytical Model Prediction

A solder bump experiences cyclic shear strain due to the differential expansion of the ceramic and the PCB. A first approximation of the cyclic strain can be obtained by considering only the deformations in the plane of the PCB. Figure 8 is a schematic of the ceramic chip-carrier mounted on the PCB.

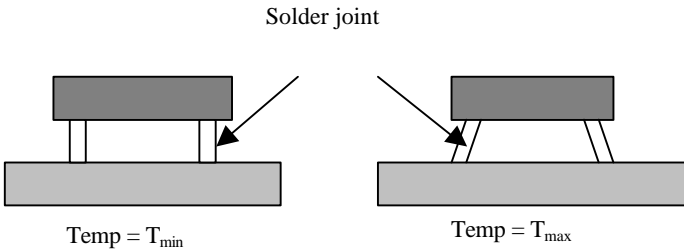


Fig. 8: Shear strain in Solder Joints

Cycles to failure for 50% of samples failed is again predicted using the Coffin-Manson relationship, however in this case, the shear strain, γ_p , is estimated from the geometry of the assembly and the mismatch in thermal expansion between the ceramic and the PCB as follows [14]:

$$g_p = \frac{L\Delta\alpha\Delta T}{2h} \quad (4)$$

Where: L = length of component
 $\Delta\alpha$ = difference in CTE
 ΔT = temperature variation
h = height of solder bump

Substituting into Equation 2 gives:

$$N_f = \frac{1}{2} \left(\frac{4he_f}{L\Delta\alpha\Delta T} \right)^m \quad (5)$$

This technique is only valid provided that the following assumptions hold [14]:

- 1) Only deformations in the plane of the PCB are considered; hence it is assumed that no bending occurs.
- 2) The chip-carrier and PCB are much stiffer than the solder joint.
- 3) Solder joint modeled as a simple column of solder, which undergoes uniform shear deformation.
- 4) Dwell times at T_{max} and T_{min} are sufficient for complete stress relaxation.
- 5) Plastic strain is equivalent to the total strain for the context of fatigue damage.

The values used in this analysis are given in Table 4. The diagonal distance from the center of the chip to the center of the corner solder ball was used for L. $\Delta\alpha$ was taken as the difference between the in-plane CTE of FR4 and the CTE of the ceramic substrate.

Table 4: Properties Used in Analytical Model

h (mm)	L (mm)	$\Delta\alpha$	ΔT (°C)	ϵ_f	M
0.89	13.47	16.1e-6	20, 35, 50	0.325	2.2

The Coffin-Manson model was used to predict the cycles to failure at 50% samples failed (Equation 5). The cycles to failure for 0.01% sample failure were then calculated using Equation 3. Sensitivity to the value of β was also investigated.

Discussion of Results

Table 5 shows N_{50} accelerated test data taken from Gerke & Kromann for the 0°C to 100°C and -40°C to 125°C cycles. Also shown in the table are the analytical and FLO/STRESS N_{50} results generated for the same ΔT and corrected to the accelerated test cycle frequencies.

Table 5: Cycles to failure; accelerated test conditions

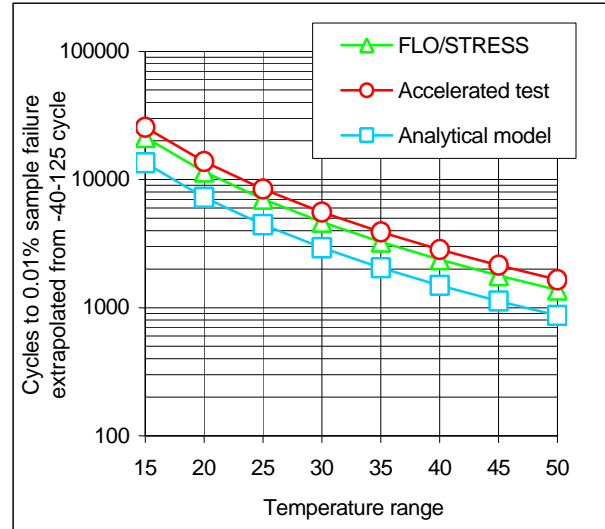
Temperature Cycle and Dwell Times	N_{50} (Cycles to 50% samples failed)		
	Accelerated Tests	Analytical Method	FLO/STRESS
0 to 100°C, 5mins	2697	2193	4190
-40 to 125°C, 15mins	1103	578	918

This is the most direct comparison that can be made with the published experimental data, providing confidence in the numerical model. The N_{50} predictions calculated using the analytical model are lower than those obtained by accelerated testing. This is as expected, since the analytical model assumes no stiffness for the solder joint and so should give a worst case figure.

In performing the above FLO/STRESS analysis, both the Pb90/Sn10 and the Sn63/Pb37 solders were strained well beyond their yield point. To correct for the use of linear elastic properties beyond the yield point, the maximum shear strains in the two solder materials were used to calculate an effective shear modulus for each material, and hence an effective elastic modulus to use to repeat the calculation. This process was repeated to convergence, requiring a total of 5 iterations.

Using the corner solder joint strain to obtain an effective elastic modulus that is then applied to all solder joints is approximately correct, since all other solder joints experience less strain, consistent with a higher effective elastic modulus. At 100°C the final maximum shear strain calculated was 1.81% in the Pb90/Sn10 solder. Since this is far in excess of the yield strain at this temperature (0.02%) it was used directly in the Coffin-Manson expression.

Under the accelerated test conditions, FLO/STRESS predicted the maximum strain to be in the corner solder joints in the Pb90/Sn10 solder, close to the eutectic solder interface. Other accelerated test studies have found the failure site to be in the Pb90/Sn10 solder, at the interface with the eutectic solder [15]. In FLO/STRESS the failure site was found to change from center of the solder joint to the package-side interface as the magnitude of the temperature cycle was reduced.



(b) Accelerated test 2 (-40°C to 125°C) (beta=6.1)

Fig. 9 (a) and (b): Cycles to failure; accelerated test conditions extrapolated to operational conditions

Figure 9 shows the temperature cycling, FLO/STRESS, and analytical model result given in Table 5, extrapolated to lower temperatures, an 8hr dwell time (assumed to provide full stress relaxation) and 0.01% sample population failure. The graph shows very similar slopes, which comes directly from the temperature dependence of the AF (Equation 1).

The calculation processes for the accelerated test and the numerical models is as follows:

Accelerated test procedure:

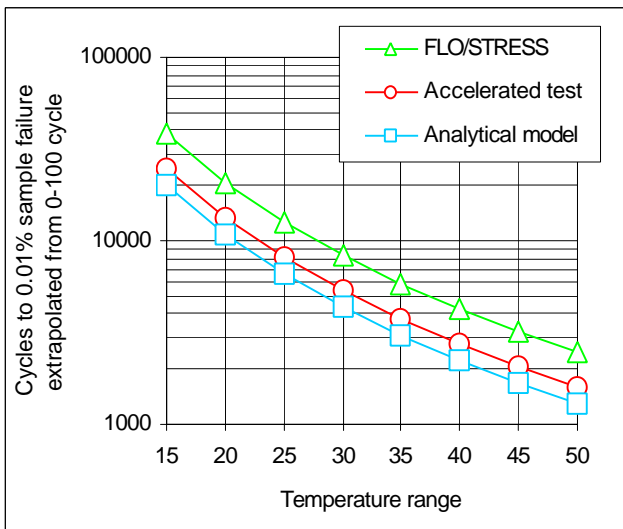
$$N_{63.2}^{15\text{min}}_{-40 \leftrightarrow 125} \xrightarrow{\text{Weibull}} N_{50}^{15\text{min}}_{-40 \leftrightarrow 125} \xrightarrow{\text{AF}} N_{50}^{8\text{hrs}}_{25 \leftrightarrow (25+\Delta T)} \xrightarrow{\text{Weibull}} N_{0.01}^{8\text{hrs}}_{25 \leftrightarrow (25+\Delta T)}$$

Numerical model procedure:

$$gT_{-40 \leftrightarrow 125}^{8\text{hrs}} \xrightarrow{C-M} N_{50}^{8\text{hrs}}_{-40 \leftrightarrow 125} \xrightarrow{\text{AF}} N_{50}^{8\text{hrs}}_{25 \leftrightarrow (25+\Delta T)} \xrightarrow{\text{Weibull}} N_{0.01}^{8\text{hrs}}_{25 \leftrightarrow (25+\Delta T)}$$

An area of uncertainty is the constants used in the Coffin-Manson equation (Equations 2 and 5). In this illustrative work representative values have been used, as data were not available for Pb90/Sn10 solder. In Figure 9(a), the N_{50} data were extrapolated to $N_{0.01}$ using the experimentally determined Weibull distribution slope for the 0°C to 100°C cycle ($\beta=9.23$). Similarly in Figure 9(b), the N_{50} data were extrapolated to $N_{0.01}$ using the experimentally determined Weibull distribution slope for the -40°C to 125°C cycle ($\beta=6.1$).

One concern about extrapolating temperature cycling data to the much lower temperatures found in real applications is the difference in material behavior between these two conditions. The properties of all the materials are temperature dependent to



(a) Accelerated test 1 (0°C to 100°C) (beta=9.23)

some degree, so the relative thermal expansion is not constant with temperature. This presents a particular problem when attempting to simulate accelerated test conditions, under which the PCB closely approaches its glass transition temperature. While it is impractical to investigate this experimentally, the solder joint strain can be calculated at the temperature and ΔT of interest using FE. The resulting strains can then be used directly in the fatigue model without temperature extrapolation.

Whereas temperature dependent properties were available for the ceramic they were not included in the calculation to avoid introducing an erroneous trend, since temperature dependent properties for the FR4 were not available. Temperature dependent properties for the solder were included. The FE analysis was re-run for ΔT s of 15°C to 50°C using a 25°C ambient, with an effective elastic modulus calculated for both solders as described above. In all cases, the maximum strain was found to be in the Pb90/Sn10 solder, so this was used in the fatigue model. For comparison purposes, the analytical model was also used to calculate cycles to failure for each temperature cycle. The calculation sequence for the numerical results is then as follows:

$$g_T \xrightarrow[25 \leftrightarrow (25 + \Delta T)]{8hrs} \xrightarrow{C-M} N_{50} \xrightarrow[25 \leftrightarrow (25 + \Delta T)]{8hrs} \xrightarrow{Weibull} N_{0.01} \xrightarrow[25 \leftrightarrow (25 + \Delta T)]{8hrs}$$

The results are shown plotted against the extrapolated accelerated test data in Figure 10. The FLO/STRESS results show a higher number of cycles to failure at lower temperatures due to the increased solder stiffness.

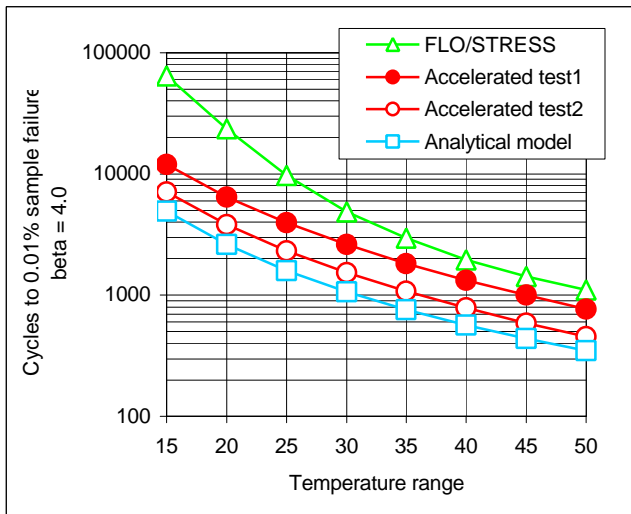


Fig. 10: Cycles to failure for operation conditions.

Another issue in using both the experimental data and the numerical results to predict the number of field returns over the expected lifetime of the equipment is that some presumption has to be made about the shape of the cumulative failure curve.

Typically this is done using a Weibull or log normal distribution. The Weibull distributions for the two temperature cycling conditions were found to have very high shape parameters of 9.23 and 6.1, indicating exacting manufacturing standards. It also indicates a highly uniform accelerated test environment.

To extrapolate to field, where equipment experiences a spectrum of conditions, lower values are appropriate, particularly if the board assembly process is being outsourced, so a Weibull slope of 4 was used in Figure 10. To illustrate the influence of the slope, Figure 11 shows the accelerated test data extrapolated to 0.01% failure using a Weibull slope of 4 [16], with error bars to indicate the spread of values obtained by using values of 3 and 8. The projected actual life is seen to depend strongly on the projection used, which itself depends on assumptions about the quality of the board assembly process.

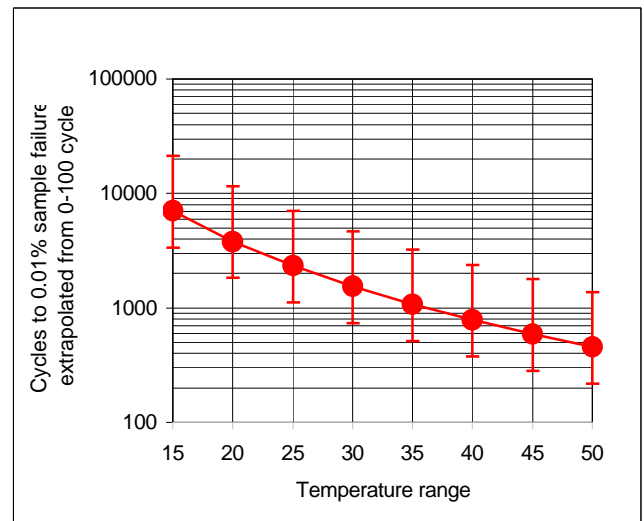


Fig. 11: Sensitivity to Weibull shape parameter

A final reason for caution when extrapolating from an accelerated test environment is that under the field conditions a temperature distribution exists within the CCA during operation. If the package and board have quite similar CTEs then most of the solder joint strain will result from the temperature difference between the package and the board. It is very difficult to include this temperature difference in an experimental accelerated test environment, and to accelerate this appropriately requires knowledge of the application environment.

CONCLUSIONS

Although the analytical model has been applied here to an isolated ceramic package with reasonable success, it is not generally applicable. In a real product, fatigue experienced by a package interconnect is highly design-dependent.

Clearly there is scope for improving the model of the solder ball in the FE analysis. However, the main modeling issue is the uncertainties regarding material property values and their temperature dependence, to which the results are very sensitive. In this illustrative study the use of representative properties in a board-level numerical model with a macro representation of the solder ball has been shown to provide adequately accurate information to allow meaningful lifetime projections to be made [17, 18, 19].

Coupled with a system-level CFD calculation, numerical simulations such as those illustrated here offer the chance to investigate the thermomechanical behavior of a package-board assembly in the application environment, where the temperature distribution within the packages and board, and mechanical interactions between packages strongly influence the reliability. The relative behavior of competing designs can be investigated with confidence by using the same material property data across all designs, and the sensitivity to any uncertainties in material property data can be investigated to build confidence in the chosen design.

Where further qualification is required, the displacements calculated for the macro model of the solder ball can be used as boundary conditions for a full visco-plastic stress-relaxation calculation for an individual solder joint using a high-end FE tool.

ACKNOWLEDGEMENTS

FLO/STRESS has been developed in conjunction with the University of Greenwich, with partial funding provided by the UK Department of Trade and Industry under a TCS Programme.

REFERENCES

[1]. "The National Technology Roadmap For Semiconductors", Semiconductor Industry Association, 1997.

[2]. J H Lau, "Thermomechanics for Electronics Packaging" in "Thermal Stress and Strain in Microelectronics Packaging", Ed. J H Lau, Van Nostran Reinhold, 1993.

[3]. "IEEE Standard Reliability Program for the Development and Production of Electronic Systems and Equipment", IEEE Reliability Society, IEEE Std. 1332-1998.

[4]. "IEEE Standard Methodology for Reliability Prediction and Assessment for Electronics Systems and Equipment" IEEE Reliability Society, IEEE Std. 1413-1998.

[5] Bailey C, Wheeler D, "Modeling Technology to Predict Flip-Chip Assembly", in Proc. ITherm 2000, IEEE No. 00CH370, pp. 79-85.

[6] Lu, H, Bailey, C, "Material Properties, Geometry and their effect on the Fatigue Life of Two Flip-Chip Components", in Proc. ITherm 2000, IEEE No. 00CH370, pp. 65-71.

[7]. Gary B. Kromann et al., "Motorola's PowerPC 603™ and PowerPC 604™ RISC Microprocessor: The C4/Ceramic-Ball-Grid Array Interconnect Technology", Proceedings of 45th Electronic Components & Technology Conference, Las Vegas, NV, May 1995, pp. 1-9.

[8]. J Zhu, K Ojala, A Tuominen, "The Application of Global/Local Technique in Finite Element Simulation of BGA Assemblies", ASME International Mechanical Engineering Congress & Exposition, Dallas, TX, 1997, pp. 1-7.

[9]. J. Parry et al., "The Development of Component-Level Thermal Compact Models of a C4/CBGA Interconnect Technology: The Motorola PowerPC 603 and 604 RISC Processors", IEEE Trans. Comp. Pack. & Man. Tech., Part A, Vol. 21, No. 1, pp. 104-112, March 1998.

[10]. "Ball Grid Array Packaging Guidelines", Jet Propulsion Laboratory, California Institute of Technology, distributed by Interconnection Technology Research Institute, August 1998.

[11] R. D. Gerke and G. B. Kromann, "Solder Joint Reliability of High I/O Ceramic-Ball-Grid Arrays and Ceramic Quad-Flat-Packs in Computer Environments: the PowerPC 603 and PowerPC 604 Microprocessors", IEEE Trans. Comp. & Pack. Tech., Vol. 22, No. 4, pp.488-496, December 1999.

[12] K. C. Norris and A. H. Landzberg, "Reliability of controlled collapse interconnections", IBM J. Res. Develop., pp. 266-271, May 1969.

[13] V. Getkin, A. Bar-Cohen and J Ames, "Coffin-Manson Fatigue Model of Underfilled Flip Chips", IEEE Trans. Comp. Pack. & Man. Tech, Part A, Vol. 20, No. 3, pp. 317-325, 1997.

[14] A. Dasgupta, "Thermomechanical Analysis and Design" in "Handbook of Electronic Package Design" Ed. M. Pecht, Marcel Dekker Inc., 1991.

[15] "Ball Grid Array Packaging Guidelines", Jet Propulsion Laboratory, California Institute of Technology, distributed by Interconnection Technology Research Institute, August 1998.

[16] W. Englemaier, "BGA and CGA Solder Attachments: Results of Low-acceleration Reliability Test and Analysis", Soldering and Surface Mount Technology, No. 24, pp. 25-31, October 1996.

[17] J. S. Corbin, "Finite element analysis for Solder Ball Connect (SBC) structural design optimisation", IBM J. Res. Develop., Vol. 37, No. 5, pp. 585-595, September 1993.

[18] H. C. Cheng, K. N. Chiang and M. H. Lee, "An Effective Approach for Three-Dimensional Finite Element Analysis of Ball Grid Array Typed Packages", ASME J. Elect. Pack., Vol. 120, pp. 129-134, June 1998.

[19] A. Syed, "ACES of Finite Element and Life Prediction Models for Solder Joint Reliability", in "Design and Reliability of Solders and Interconnects", Eds. R. Mahidhara, D. Frear, S. Sastry, K. Murty, P. Liaw and W. Winterbottom, TMS 1997.